

## Abstract

The water Cherenkov detector array (WCDA), sub-array of Large High Altitude Air Shower Observatory (LHAASO), is highly sensitive to VHE gamma-ray and is dedicated to surveying the northern sky (100GeV to 30TeV). In this work, the Mrk421 is monitored over period from 2019 July to 2020 February with the first detector array of WCDA. The significance and excess over background of this source are measured for this period and will compare with the observation by the satellite-borne experiment Fermi in the GeV range. The evolution of the spectral energy distribution is also investigated by measuring spectral indices at two different flux levels.

## 1. Introduction

Mrk421(z=0.031) is one of the closest and brightest blazars known and is classified as a BL Lac object, a subclass of active galactic nuclei (AGNs). It is a galaxy with a strong and variable non-thermal emission. which is believed to be the result of the accretion of supermassive black hole lying at the center of the galaxy, the model of AGN is shown in Fig.1 (Left). Blazars are a broadband continuum ranging from radio through x-ray to gamma-ray.

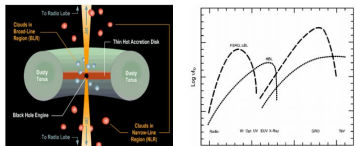


Fig. 1: Left: The model structure of Active Galactic Nuclei. Right: Broad-band energy spectrum from radio to TEV gamma-ray

The spectral energy distributions (SEDs) are characterized by two distinct bumps, as shown in Fig.1(Right). The lower energy component, which peaks in the optical through x-ray, is caused by the synchrotron radiation from relativistic electrons (and positrons) within the jet, the origin of the hump at higher energy is under debate

## 2. Experimental set-up

The Water Cherenkov Detector Array (WCDA), covering an area of 78,000m<sup>2</sup>, has been built in three phases, more details about the detector are shown in Fig. 2 (Right). WCDA is able to survey the TeV sky for steady and transit sources from 100GeV-30TeV with a large field of view (FOV), full duty circle, good angular resolution and fine gamma/proton identification.

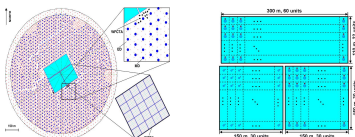


Fig. 2: Left: The layout of the LHAASO experiment. LHAASO consists of one square kilometer array (KM2A), Water Cherenkov detector array (WCDA) and wide-field Cherenkov telescope array (WFCTA). Right: Schematic of the WCDA layout.

WCDA mainly focuses on very high energy gamma astronomy. Through the observation of very high energy, it will help to understand the origin of cosmic rays and the internal activities of extreme celestial bodies.

## 3. Analysis Methods

### 3.1 The Data Selection

All events are collected in the period from Jul. 1, 2019 to Feb. 29, 2020 around the Mrk421 direction are grouped into four bins of N<sub>file</sub>, namely [60, 100], [100, 200], [200-300] and [300, 800]. Moreover, the criteria for events to be used in the analysis are as follows. All the criteria helped to maximize the detection significance.

- (I) 60 ≤ N<sub>file</sub> < 800.
- (II) The Mrk421 was at least 50 degree above the horizon.
- (III) The compactness is larger than 15.

### 3.2 Cosmic-Ray Background Suppression

To maximize the sensitivity to gamma-ray showers, the background suppression is important. One of the most powerful gamma/proton separation techniques is define a parameter named compactness. The compactness is defined as C=Nhit/Max(Qi;r >Rc). For WCDA-1, the C>15 is optimal to distinguish the muon signal. The result is shown in Fig. 3, the left one is the compactness distribution of gamma and proton, the right one is distribution of Q, a parameter used to measure the level of particle identification.

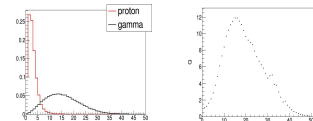


Fig. 3: (Left) The compactness distribution of proton and gamma. (Right) The distribution of Q factor.

### 3.3 Cosmic-Ray Background Estimation

We select an area of 5 degree × 5 degree, centered at the Mrk421 direction, covered it with a grid with a cell size of 0.1 degree × 0.1 degree, after converting the information of the particles from local coordinates to equatorial coordinates. In order to calculate the excess of signals from Mrk421 direction, we use direct integration to obtain a background estimate. This method is based on the assumption that acceptance of the detector, in local coordinates, is independent of the trigger rate over a period of two hours and that the cosmic ray background is isotropic.

## 4. Results for Mrk421

### 4.1 Flux Light Curve

The light curves of WCDA and Fermi-LAT, as shown in Fig. 4. In the result of WCDA, we use the signals characterize the current flux variations considering the energy. From the result, we find that the GeV gamma-ray flux appears to be moderately correlated with the TeV gamma-ray.

From 2019 August (MJD=58720) to 2019 September (MJD=58729) and 2020 February (MJD=58881) to 2020 February (MJD=58899), Mrk421 shows high activity in the two bands, we mark this period as a flaring phase, and the duration is 5.44 × 10<sup>5</sup> s, The other days are marked as a steady phase and the duration is 5.38 × 10<sup>6</sup> s.

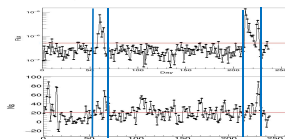


Fig. 4 Mrk421 light curves in different bands, from 2019 July 1 to 2020 February 29. The upper one is the result of Fermi-LAT, each bin of it contains the event every day. The lower one represents the result of WCDA and each bin of it contains the event averaged 3 days.

### 4.2 Spectre Energy Distribution of Mrk421

Based on section 3, the significance, number of excess events in each bin are calculated by the Maximum Likelihood method. The result of the two different Phases are listed in Table 1 (the left one represents the steady phase and the right one represents the flaring phase), and Fig. 5 only shows the significance maps and excess of the energy range [200-300].

Table 1. Summary of data used in the measurement of SED of Mrk421

N <sub>hit</sub>	E <sub>median</sub> (TeV)	Excess	sig
60-100	0.62	1382.62	9.9
100-200	1.45	821.50	16.3
200-300	3.41	214.11	11.7
300-800	7.27	57.17	7.4

N <sub>hit</sub>	E <sub>median</sub> (TeV)	Excess	sig
60-100	0.60	122.45	4.2
100-200	1.41	98.90	5.8
200-300	3.34	9.70	3.1
300-800	7.11	20.84	6.9

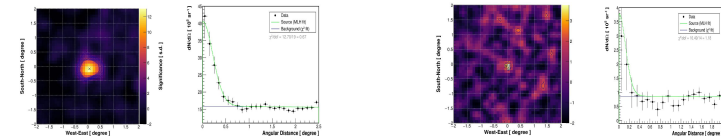


Fig. 5 The result of the significance map and the excess in the different phases. (Left) represents the steady phase. (Right) represents the flaring phases.

The SED is determined by minimizing the X<sup>2</sup> function

$$X^2 = \sum_{i=1}^4 \frac{[N_i^{obs} - N_i^{exp}(\phi_0, \alpha, \beta)]^2}{(\sigma_i^{obs})^2} \quad (1)$$

The excess is the expected number of events according to the hypothesis of a log-parabolic model

$$\phi(E) = \left(\frac{E}{3TeV}\right)^{-\alpha - \beta \ln\left(\frac{E}{3TeV}\right)} \quad (2)$$

The SED measured using WCDA-1 is shown in Fig. 6. The energy of each point is the gamma-ray median energy for the corresponding N<sub>file</sub> interval. The red points represents the steady phase, the spectral parameters obtained in the log-parabolic fitting are shown in Table 2.

Table 2. The result of different phases on Mrk421

phase	φ <sub>0</sub> (TeV <sup>-1</sup> cm <sup>-2</sup> s <sup>-1</sup> )	α
steady phase	4.80 ± 0.37	3.13 ± 0.092
flaring phase	4.13 ± 1.13	3.18 ± 0.28

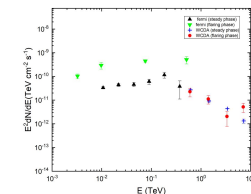


Fig. 6: The SED of the Mrk421

## 5. Summary and Outlook

- (I) The time correlation among the flux variation in different wavebands was analyzed. The variation of GeV gamma-ray is roughly correlated with the TeV gamma-ray.
- (II) It is found that there is no distinct difference in the energy spectrum index between the two periods. The energy index in the steady phase is -3.13 and in the flaring phase is -3.18.
- (III) Use the full array of data and increase the data sample, and divide the flaring period more carefully according to different flux variation to complete the measurement of Mrk421 energy spectrum distribution.

## 6. Reference

- [1] MILAGRO Collaboration, APJ, 595 (2) (2003) 803-811.
- [2] B. Bartoli, et al., The Astrophysical Journal Supplement Series, 222:6 (17pp), 2016 January.
- [3] Randall L. Oglisby, Modeling the spectral Energy Distribution of Mrk421. (2013)